Electronic Supplementary Information

A luminescent linear trinuclear Dy^{III} complex exhibiting slow magnetic relaxation of single ion origin

Chun-Sen Liu,[a] Miao Du,[,b] E. Carolina Sañudo,[*,c] Min Hu,[a] Qiang Zhang,[a] Jorge Echeverria,[c] Li-Ming Zhou[a] and Shao-Ming Fang[*,a]*

[a] *Zhengzhou University of Light Industry, Henan Provincial Key Laboratory of Surface & Interface Science, Zhengzhou, Henan 450002, China*

[b] *College of Chemistry, Tianjin Key Laboratory of Structure and Performance for Functional Molecule, Tianjin Normal University, Tianjin 300387, China*

[c] *Institut de Nanociència i Nanotecnologia i Departament de Química Inorgànica, Universitat de Barcelona, Diagonal, 647, 08028-Barcelona, Spain*

* To whom correspondence should be addressed. E-mail addresses: smfang@zzuli.edu.cn (S.-M.F.); dumiao@public.tpt.tj.cn (M.D.); carolina.sanudo@qi.ub.es (E.C.S.)

Dalton Trans.

Experimental section

Materials and general methods

All the starting reagents and solvents for synthesis and analysis were commercially available and used as received. Elemental analyses were performed on a Vario EL III Elementar analyzer. IR spectra were taken in 4000–400 cm^{-1} on a Tensor 27 OPUS (Bruker) FT-IR spectrometer with KBr pellets. Thermogravimetric analysis (TGA) experiments were carried out on a Perkin-Elmer Diamond SII thermal analyzer from room temperature to 1000 °C under N_2 atmosphere at a heating rate of 10 °C/min. The emission and excitation fluorescent spectra were recorded on an F-7000 (Hitachi) spectrophotometer at room temperature in solid state.

Single crystal X-ray diffraction data were collected using a Bruker Smart 1000 CCD area-detector diffractometer with Mo-Kα radiation (λ = 0.71073 Å) by ω scan mode. The program SAINT was used for integration of the diffraction profiles. Semi-empirical absorption corrections were applied using SADABS. The structures were solved by direct methods using the SHELXS program of the SHELXTL package and refined by full-matrix least-squares methods with SHELXL. Metal atoms were located from the *E*-maps and the other non-hydrogen atoms were located in successive difference Fourier syntheses and refined with anisotropic thermal parameters on F^2. The carbon-bound hydrogen atoms were generated theoretically and refined with isotropic thermal parameters riding on the parent atoms.

Powder X-ray diffraction (PXRD) patterns were recorded on a Bruker D8 Advance diffractometer at 40 kV and 100 mA, by using a Cu-target tube (λ = 1.54056 Å) and a graphite monochromator. The powder samples were prepared by crushing the large single crystals and the intensity data were recorded by continuous scan in a $2\theta/\theta$ mode from 3° to 40° with a step size of 0.02° and a scan speed of 8 °/min. Simulation of the PXRD patterns was carried out by the single-crystal data and diffraction-crystal module of the *Mercury* (Hg) program.

Magnetic measurements were performed in the Unitat de Mesures Magnètiques (Universitat de Barcelona) on crushed polycrystalline samples (ca. 30 mg) with a Quantum Design SQUID MPMS-XL mag-

netometer equipped with a 5 T magnet. Diamagnetic corrections were calculated using Pascal's constants and an experimental correction for the sample holder was applied.

Syntheses of 1 and 2

A mixture of Dy_2O_3 (0.2 mmol, 0.0746 g) or Gd_2O_3 (0.2 mmol, 0.0725 g), salicylic acid (H_2**SA**, 1.6 mmol, 0.2210 g), 1,10-phenanthroline (phen, 0.4 mmol, 0.0721 g), and distilled H_2O (15 mL) was sealed in a 23-mL stainless steel reactor with a Teflon liner and heated in an oven at 140 °C for 4 days and then cooled to room temperature at a rate of 5 °C h^{-1}. Yellow block crystals for complexes **1** or **2** suitable for X-ray structural analysis were washed with ethanol-ether and then dried in air (yield: ca. 40% based on H_2**SA**). Elemental analysis calcd (%) for $C_{85}H_{57}Dy_3N_6O_{21}$ (**1**): C 51.41, H 2.89, N 4.23; found (%): C 51.64, H 2.97, N 4.39. IR for **1** (cm^{-1}): ν = 3425(br, m), 1627(m), 1601(s), 1570(s), 1513(m), 1466(s), 1420(m), 1386(s), 1333(m), 1310(w), 1249(m), 1221(w), 1144(m), 1103(w). 1050(w), 1032(w), 956(w), 891(w), 865(m), 846(m), 807(w), 758(m), 730(m), 705(w), 664(m), 605(w), 579(w), 553(w), 536(w), 466(w). Elemental analysis calcd (%) for $C_{85}H_{57}Gd_3N_6O_{21}$ (**2**): C 51.82, H 2.92, N 4.27; found (%): C 51.71, H 3.04, N 4.42. IR for **2** (cm^{-1}): ν = 3430(br, m), 1627(m), 1600(s), 1568(s), 1511(m), 1465(s), 1421(m), 1385(s), 1333(m), 1310(w), 1249(m), 1221(w), 1143(m), 1102(w), 1049(w), 1032(w), 956(w), 889(w), 865(m), 845(m), 807(w), 758(m), 730(m), 706(w), 664(m), 603(w), 579(w), 553(w), 536(w), 466(w).

Table S1 Crystallographic data and structural refinement summary for complexes **1** and **2**

	1	**2**
empirical formula	$C_{85}H_{57}Dy_3N_6O_{21}$	$C_{85}H_{57}Gd_3N_6O_{21}$
formula weight	1985.87	1970.12
crystal system	Monoclinic	Monoclinic
space group	$P2_1/c$	$P2_1/c$
unit cell dimensions (Å, °)		
a	14.2574(7)	14.3190(2)
b	23.3393(10)	23.3948(3)
c	23.6971(14)	23.7896(4)
β	103.294(6)	103.405(2)
volume (Å^3)	7674.1(7)	7752.2(2)
Z	4	4
D_{calcd} (g/cm^3)	1.719	1.688
μ (mm^{-1})	2.972	2.617
Crystal size (mm^3)	0.25 × 0.19 × 0.18	0.25 × 0.19 × 0.14
F(000)	3900	3876
range of h, k, l	–16/15, –27/27, –28/28	–17/16, –26/27, –27/28
reflections collected/unique/observed	53714/13494/8625	52328/13636/10012
max. & min. transmission	0.6168 & 0.5237	1.0000 & 0.84571
data/restraints/parameters	13494/18/1024	13636/6/1024
R_{int}	0.0658	0.0322
T (K)	294(2)	294(2)
goodness-of-fit on F^2	1.017	0.911
R_1[a] & wR_2[b] [$I > 2\sigma(I)$]	0.0333 & 0.0450	0.0238 & 0.0554
R_1[a] & wR_2[b] (all data)	0.0700 & 0.0474	0.0388 & 0.0570
largest diff. peak & hole (e/Å^3)	1.549 & –0.764	2.277 & –0.548

[a] $R_1 = \Sigma(||F_o| - |F_c||)/\Sigma|F_o|$; [b] $wR_2 = [\Sigma w(|F_o|^2 - |F_c|^2)^2/\Sigma w(F_o^2)^2]^{1/2}$.

Table S2 Selected bond distances (Å) and angles (°) for complexes **1** and **2**

1

Dy1–O12	2.172(3)	Dy1–O7	2.275(4)
Dy1–O1	2.319(3)	Dy1–O11	2.371(4)
Dy1–O4	2.407(3)	Dy1–O5	2.444(4)
Dy1–N1	2.579(5)	Dy1–N2	2.614(4)
Dy2–O18	2.170(3)	Dy2–O13	2.281(4)
Dy2–O19	2.318(3)	Dy2–O17	2.362(3)
Dy2–N5	2.562(4)	Dy2–N6	2.567(4)
Dy2–N3	2.575(5)	Dy2–N4	2.615(4)
Dy3–O14	2.294(3)	Dy3–O20	2.303(4)
Dy3–O2	2.319(4)	Dy3–O8	2.332(3)
Dy3–O16	2.363(4)	Dy3–O10	2.380(3)
Dy3–O11	2.421(3)	Dy3–O17	2.481(3)
O12–Dy1–O7	146.90(14)	O12–Dy1–O1	97.23(12)
O7–Dy1–O1	88.24(13)	O12–Dy1–O11	73.55(13)
O7–Dy1–O11	76.03(12)	O1–Dy1–O11	76.87(12)
O12–Dy1–O4	106.30(13)	O7–Dy1–O4	84.22(13)
O1–Dy1–O4	147.40(12)	O11–Dy1–O4	131.04(12)
O12–Dy1–O5	81.90(13)	O7–Dy1–O5	79.52(13)
O1–Dy1–O5	154.47(14)	O11–Dy1–O5	78.46(12)
O4–Dy1–O5	53.87(13)	O12–Dy1–N1	74.01(14)
O7–Dy1–N1	138.83(13)	O1–Dy1–N1	90.29(13)
O11–Dy1–N1	143.11(12)	O4–Dy1–N1	75.31(14)
O5–Dy1–N1	113.64(13)	O12–Dy1–N2	135.04(15)
O7–Dy1–N2	77.72(14)	O1–Dy1–N2	72.28(12)
O11–Dy1–N2	139.71(13)	O4–Dy1–N2	75.13(12)
O5–Dy1–N2	125.62(13)	N1–Dy1–N2	62.76(14)

O18–Dy2–O13	146.83(13)	O18–Dy2–O19	105.03(12)
O13–Dy2–O19	88.62(13)	O18–Dy2–O17	74.53(12)
O13–Dy2–O17	80.95(12)	O19–Dy2–O17	73.44(11)
O18–Dy2–N5	89.74(13)	O13–Dy2–N5	95.04(14)
O19–Dy2–N5	146.63(13)	O17–Dy2–N5	139.90(12)
O18–Dy2–N6	83.19(13)	O13–Dy2–N6	69.92(13)
O19–Dy2–N6	146.50(14)	O17–Dy2–N6	77.86(12)
N5–Dy2–N6	63.58(14)	O18–Dy2–N3	76.48(14)
O13–Dy2–N3	136.68(13)	O19–Dy2–N3	73.23(13)
O17–Dy2–N3	127.56(12)	N5–Dy2–N3	81.72(14)
N6–Dy2–N3	139.70(14)	O18–Dy2–N4	138.01(15)
O13–Dy2–N4	74.38(14)	O19–Dy2–N4	74.82(12)
O17–Dy2–N4	139.89(13)	N5–Dy2–N4	74.32(13)
N6–Dy2–N4	120.56(13)	N3–Dy2–N4	63.10(15)
O14–Dy3–O20	87.20(13)	O14–Dy3–O2	71.91(13)
O20–Dy3–O2	84.53(14)	O14–Dy3–O8	148.94(12)
O20–Dy3–O8	77.15(12)	O2–Dy3–O8	79.94(13)
O14–Dy3–O16	132.22(13)	O20–Dy3–O16	91.47(13)
O2–Dy3–O16	155.44(12)	O8–Dy3–O16	75.54(12)
O14–Dy3–O10	79.96(13)	O20–Dy3–O10	150.40(13)
O2–Dy3–O10	115.89(14)	O8–Dy3–O10	125.34(13)
O16–Dy3–O10	78.17(14)	O14–Dy3–O11	104.51(12)
O20–Dy3–O11	155.64(11)	O2–Dy3–O11	79.14(13)
O8–Dy3–O11	82.25(12)	O16–Dy3–O11	95.89(12)
O10–Dy3–O11	53.93(12)	O14–Dy3–O17	79.86(12)
O20–Dy3–O17	76.77(12)	O2–Dy3–O17	146.75(12)
O8–Dy3–O17	121.15(12)	O16–Dy3–O17	53.58(11)
O10–Dy3–O17	74.78(12)	O11–Dy3–O17	125.82(10)
Dy1–O11–Dy3	131.69(13)	Dy2–O17–Dy3	130.51(13)
Dy1–Dy3–Dy2	165.34(1)		

2

Gd1–O12	2.207(2)	Gd1–O7	2.314(2)
Gd1–O1	2.338(3)	Gd1–O11	2.405(3)
Gd1–O4	2.429(3)	Gd1–O5	2.471(3)
Gd1–N1	2.610(3)	Gd1–N2	2.633(3)
Gd2–O18	2.202(3)	Gd2–O13	2.318(2)
Gd2–O19	2.344(3)	Gd2–O17	2.381(2)
Gd2–N6	2.597(3)	Gd2–N5	2.601(3)
Gd2–N3	2.605(3)	Gd2–N4	2.642(3)
Gd3–O14	2.331(3)	Gd3–O20	2.350(2)
Gd3–O8	2.362(3)	Gd3–O2	2.362(3)
Gd3–O16	2.396(3)	Gd3–O10	2.425(3)
Gd3–O11	2.447(2)	Gd3–O17	2.512(2)

O12–Gd1–O7	146.64(10)	O12–Gd1–O1	97.39(10)
O7–Gd1–O1	87.85(10)	O12–Gd1–O11	72.65(9)
O7–Gd1–O11	76.60(9)	O1–Gd1–O11	76.88(9)
O12–Gd1–O4	106.32(10)	O7–Gd1–O4	84.39(9)
O1–Gd1–O4	147.55(10)	O11–Gd1–O4	131.01(10)
O12–Gd1–O5	81.85(11)	O7–Gd1–O5	79.97(10)
O1–Gd1–O5	155.06(10)	O11–Gd1–O5	79.15(10)
O4–Gd1–O5	53.04(10)	O12–Gd1–N1	74.52(10)
O7–Gd1–N1	138.64(10)	O1–Gd1–N1	89.90(10)
O11–Gd1–N1	142.48(9)	O4–Gd1–N1	75.82(10)
O5–Gd1–N1	113.58(10)	O12–Gd1–N2	135.38(10)
O7–Gd1–N2	77.59(10)	O1–Gd1–N2	72.17(10)
O11–Gd1–N2	140.04(9)	O4–Gd1–N2	75.39(10)
O5–Gd1–N2	125.18(10)	N1–Gd1–N2	62.52(10)
O18–Gd2–O13	146.83(9)	O18–Gd2–O19	104.13(10)
O13–Gd2–O19	89.39(10)	O18–Gd2–O17	73.75(9)

O13–Gd2–O17	81.52(8)	O19–Gd2–O17	73.75(8)
O18–Gd2–N6	83.70(10)	O13–Gd2–N6	69.50(10)
O19–Gd2–N6	146.68(9)	O17–Gd2–N6	77.73(9)
O18–Gd2–N5	89.76(10)	O13–Gd2–N5	94.88(10)
O19–Gd2–N5	147.23(9)	O17–Gd2–N5	139.02(9)
N6–Gd2–N5	63.10(9)	O18–Gd2–N3	76.45(10)
O13–Gd2–N3	136.72(9)	O19–Gd2–N3	73.17(9)
O17–Gd2–N3	127.66(8)	N6–Gd2–N3	139.57(10)
N5–Gd2–N3	81.76(9)	O18–Gd2–N4	137.63(10)
O13–Gd2–N4	74.81(9)	O19–Gd2–N4	75.28(10)
O17–Gd2–N4	140.87(10)	N6–Gd2–N4	120.43(10)
N5–Gd2–N4	74.58(10)	N3–Gd2–N4	62.64(10)
O14–Gd3–O20	86.95(10)	O14–Gd3–O8	148.86(11)
O20–Gd3–O8	76.74(9)	O14–Gd3–O2	71.97(10)
O20–Gd3–O2	85.54(10)	O8–Gd3–O2	80.36(10)
O14–Gd3–O16	131.74(10)	O20–Gd3–O16	91.23(10)
O8–Gd3–O16	75.70(10)	O2–Gd3–O16	155.94(10)
O14–Gd3–O10	80.11(11)	O20–Gd3–O10	150.53(10)
O8–Gd3–O10	125.62(10)	O2–Gd3–O10	114.79(11)
O16–Gd3–O10	78.33(11)	O14–Gd3–O11	104.96(9)
O20–Gd3–O11	156.58(9)	O8–Gd3–O11	83.12(8)
O2–Gd3–O11	79.35(9)	O16–Gd3–O11	95.32(9)
O10–Gd3–O11	52.82(9)	O14–Gd3–O17	80.12(9)
O20–Gd3–O17	76.60(8)	O8–Gd3–O17	120.38(8)
O2–Gd3–O17	147.54(9)	O16–Gd3–O17	52.78(8)
O10–Gd3–O17	75.16(9)	O11–Gd3–O17	124.75(8)
Gd1–O11–Gd3	130.53(11)	Gd2–O17–Gd3	129.66(10)
Gd1–Gd3–Gd2	165.41(1)		

Table S3 Continuous shape measures for the three Dy^{III} ions in **1***

metal center	coordination sphere	**SAPR**	**DD**	**BTP**
Dy1	DyO_6N_2	3.725	**2.323**	**2.393**
Dy2	DyO_4N_4	**1.917**	**1.392**	2.148
Dy3	DyO_8	3.025	**2.083**	3.252

***** A smaller the shape measure, the closer the coordination polyhedron is to the ideal shape. SAPR: square anti-prism (D_4d); DD: triangular dodecahedron (D_2d), BTP: biaugmented trigonal prism (C_2v). The bold numbers indicate the best coincidence.

Table S4 Parameters for weak interactions (Å, °) in **1**

D–H···A	$d_{D\cdots A}$	$d_{H\cdots A}$	$\angle_{D-H\cdots A}$	symmetry code
C52–H52A···O9	2.513(7)	3.37	154	$x-1, y, z$
C63–H63A···O12	2.455(4)	3.36	166	$x+1, y, z$
C64–H64A···O15	2.571(6)	3.31	137	$x+1, y, z$
C51–H51A···*Cg*1*	2.927(1)	3.81	159	$-x-1, y-1/2, -z+3/2$
C75–H75A···O6	2.515(7)	3.23	134	$-x+1, y+1/2, -z+3/2$
C13–H13A···*Cg*2*	2.942(1)	3.86	170	$x, y-1, z$
C12–H12A···*Cg*3*	3.042(2)	3.93	160	$x, y-1, z$
C26–H26A···*Cg*4*	3.241(3)	3.99	139	$x, y-1/2, z+1/2$
C47–H47A···*Cg*1*	2.659(5)	3.56	163	$x, y-1/2, z-1/2$
C55–H55A···*Cg*5*	3.065(8)	3.82	139	$x-1, -y+1/2, z-1/2$

* *Cg*1, *Cg*3, and *Cg*4 are the centroids of the C37–C42, C23–C28, and C2–C7 phenyl rings of **SA** and H**SA** ligands in **1**, respectively; *Cg*2 and *Cg*5 are the centroids of the C62–C65/N3/C73 and C80–C84/N10 pyridyl rings of phen ligands in **1**, respectively. All the data were calculated by the PLATON program.

Table S5 Structural features and magnetic coupling of some related Dy^{III} complexes

	Dy···Dy (Å)	**Dy-O-Dy (°)**	**bridging ligands**	**coupling***	**ref.**
$[Dy_3(C_7H_4O_3)_2(C_7H_5O_3)_5(phen)_3]$	4.372 4.398	131.55 130.47	μ-O, 2 μ-RCO_2^-	F	this work
$[Dy_2Co_2(2,5\text{-}pydc)H_2O)_4]_n$	4.487	129.76	μ-O, 2 μ-RCO_2^-	F	28
$[Dy_2(H_2O)_2(C_{14}H_8O_4)_3]_n$	4.440	124.35	μ-O, 2 μ-RCO_2^-	U	29
$[Dy_4(L)_4(MeOH)_6]$	------	149.99	3 μ-O	F	30

* F: ferromagnetic coupling; U: uncoupling.

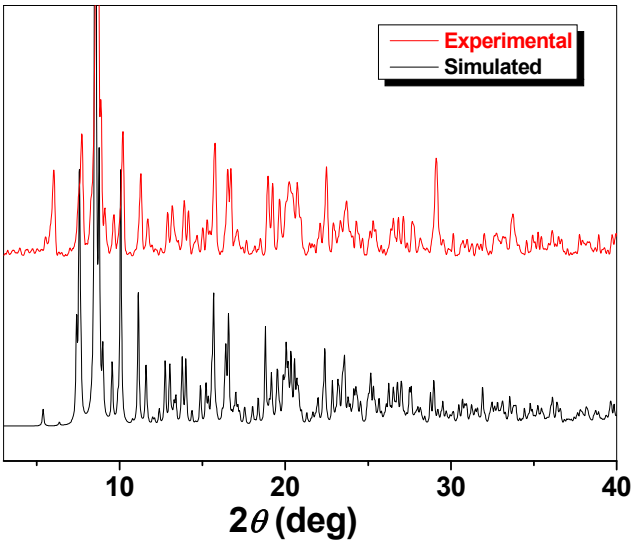

(a)

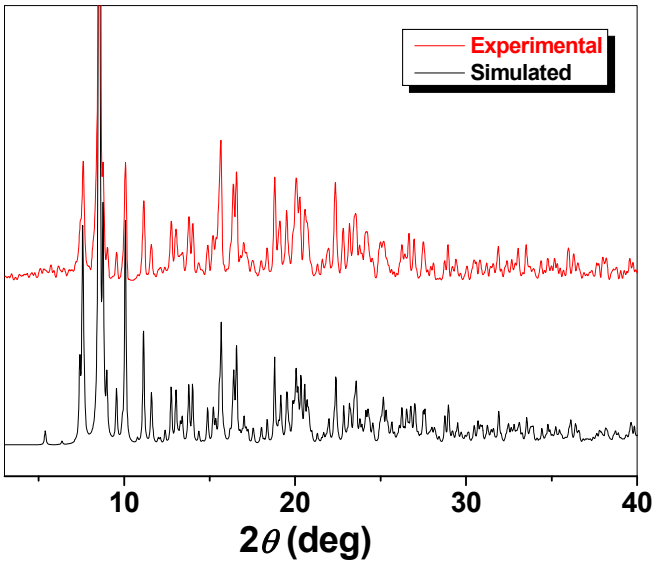

(b)

Fig. S1 Powder X-ray diffraction (PXRD) patterns for (a) **1** and (b) **2**.

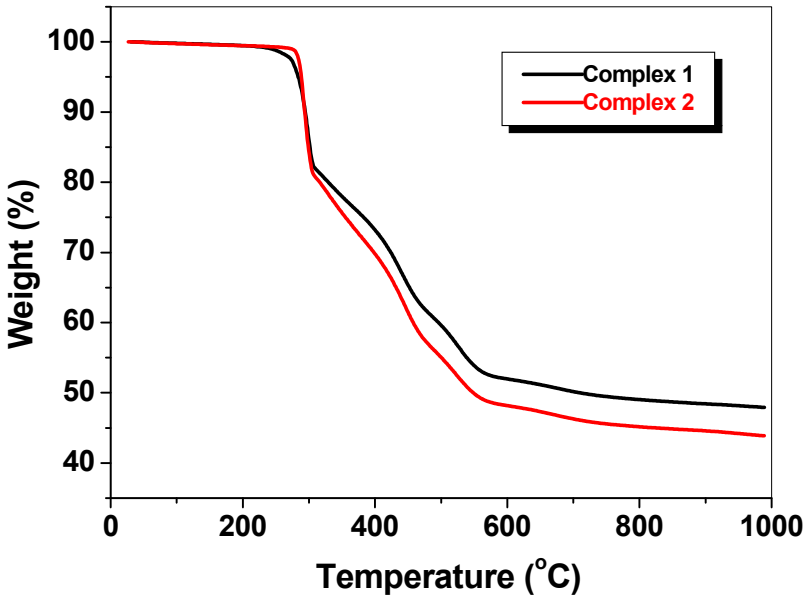

Fig. S2 Thermogravimetric analysis (TGA) traces for (a) **1** and (b) **2**.

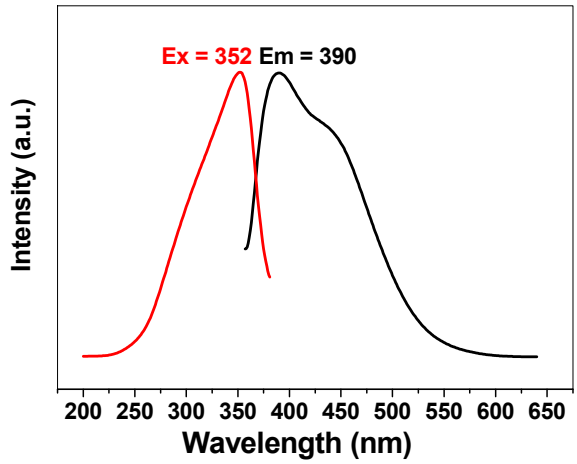

(a)

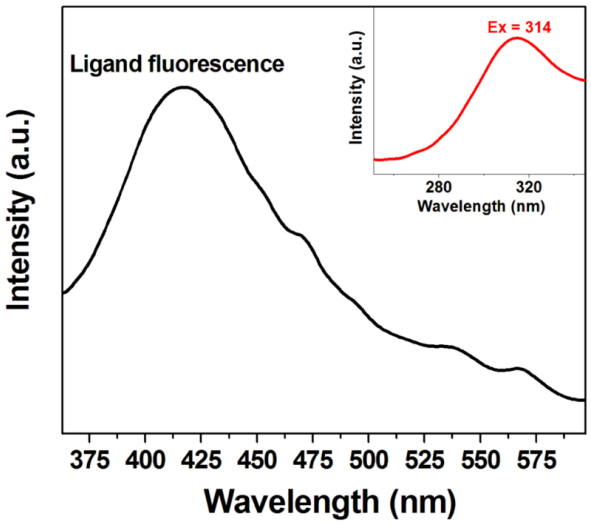

(b)

Fig. S3 Solid-state excitation/emission spectra for (a) the H_2**SA** ligand and (b) complex **2**.

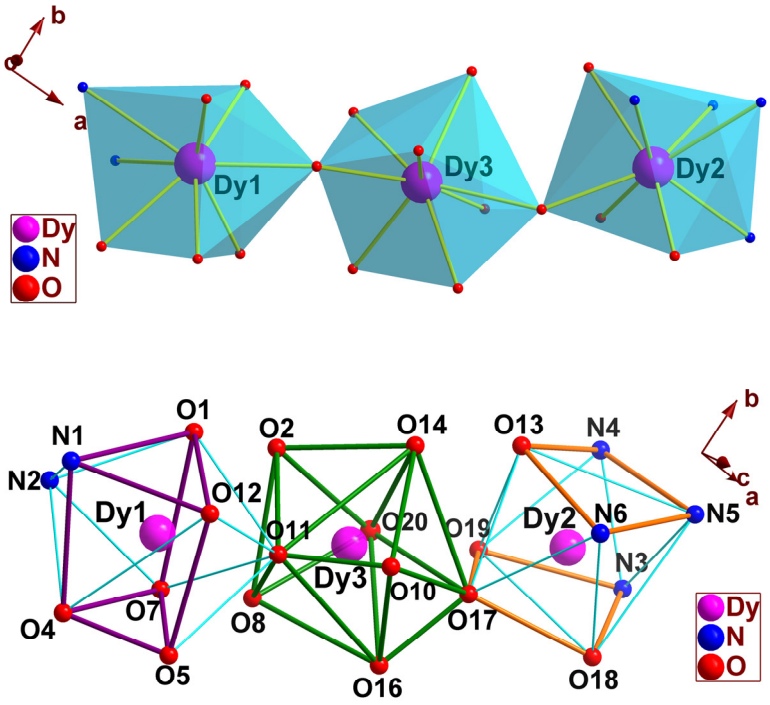

Fig. S4 Coordination polyhedra observed for the three Dy^{III} centers in **1**.

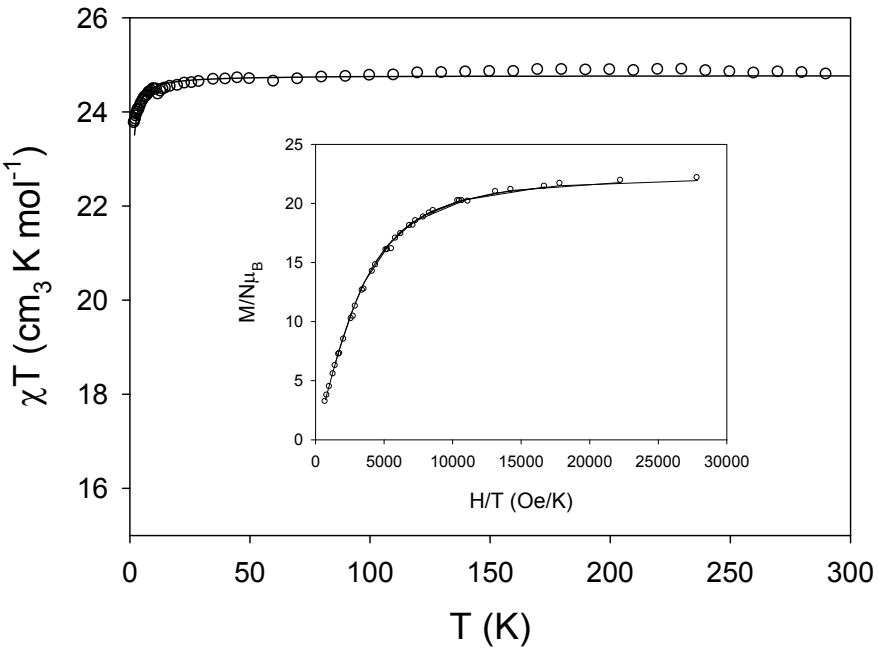

Fig. S5 χT vs. T plot for **2** at an applied dc field of 0.3 T, from 300 K to 30 K and applied fields of 0.3 T and 200 Oe below 30 K. The solid line is the best fitting to the experimental data. The inset shows a reduced magnetization plot at temperatures between 7 and 1.8 K and applied fields between 0 and 5 T; the solid line is the Brillouin function for three isolated S = 7/2 Gd^{III} ions with g = 2.10.

Results and discussion

The χT product of **2** is 24.7 cm^3 K mol^{-1} at 300 K, slightly above the expected 23.6 cm^3 K mol^{-1} for three uncoupled Gd^{III} ions ($^8S_{7/2}$, S = 7/2, L = 0, g = 2.0). The χT product follows the Curie law until at temperatures below 10 K, and it slightly drops to a value of 23.7 cm^3 K mol^{-1} at 2 K. This clearly indicates that the magnetic exchange between the three Gd^{III} centers in **2** is very weak and in the temperature range studied the three ions are practically isolated. An analytical Van Vleck equation can be written using the equivalent operator approach and the following Hamiltonian:

$$\hat{H} = -2J1[\hat{S}1\cdot\hat{S}2 + \hat{S}2\cdot\hat{S}3] - 2J2[\hat{S}1\hat{S}3]$$

where $\hat{S}1$, $\hat{S}2$ and $\hat{S}3$ refer to Gd1, Gd2 and Gd3. $J2$ was fixed at a value of zero due to the long distance between Gd1 and Gd3 (d = 8.73 Å), and the best fitting parameters where $|J1|$ = 0.005 cm^{-1} and g = 2.05.

The *J* value is very small, and the fitting is slightly better if *J* is positive but similar fittings can be obtained with *J* negative. Taking the ferromagnetic coupling (*J* positive) leads to a ground state of $S_T = 21/2$, with all the possible exited states in a range of less than 1 cm^{-1}. Thus, from these data, we can conclude that the three Gd^{III} ions are magnetically isolated in the temperature range studied here. This can also be reflected in the reduced magnetization plot, even at low temperatures, there is Boltzman population of all the possible spin states. The superposition of the isofield lines into one master curve reflects the lack of anisotropy of **2** and the data follow the Brillouin law (shown as the solid line) for three isolated S = 7/2 Gd^{III} ions. There is no sign of any slow relaxation process in the ac magnetic susceptibility.

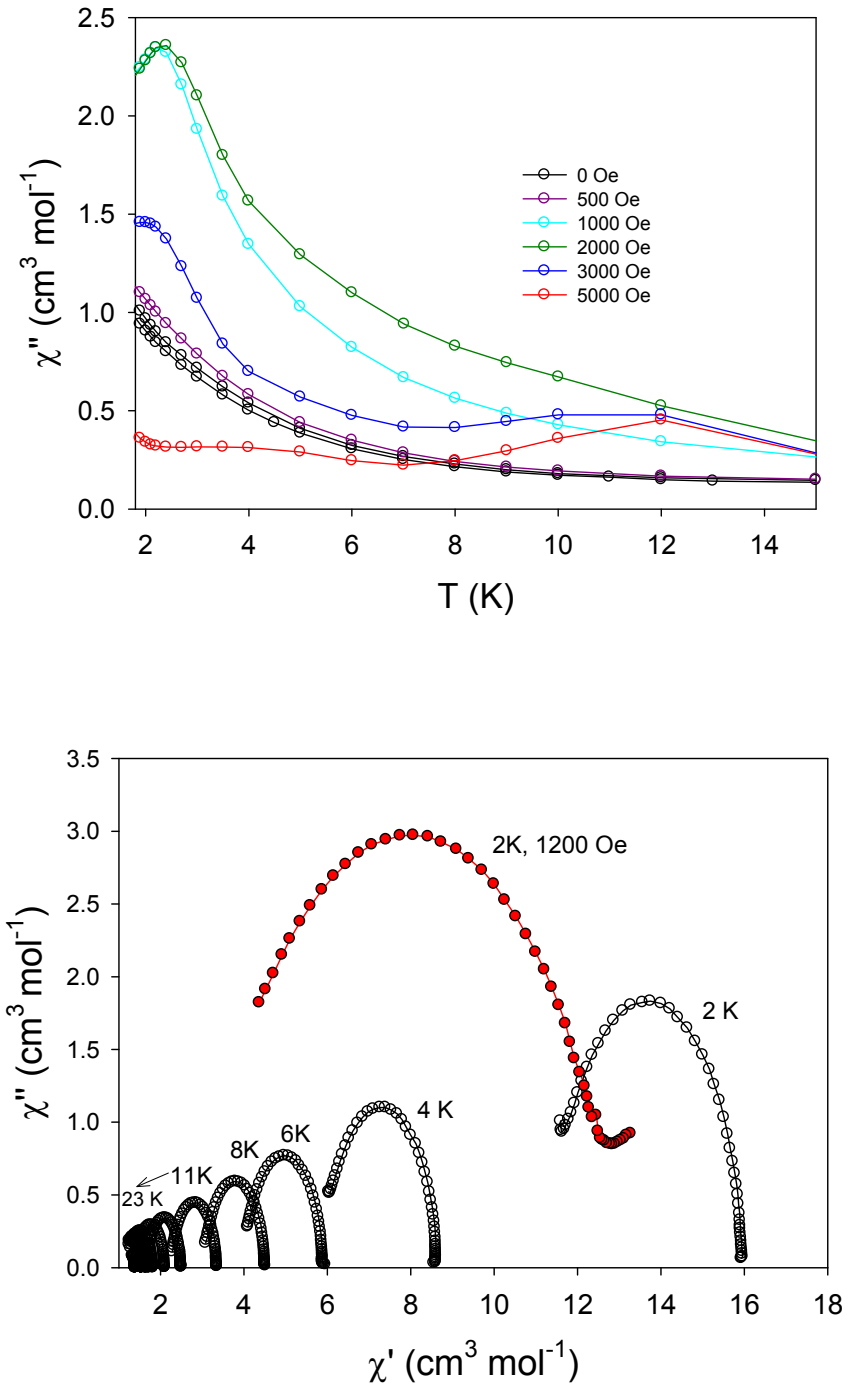

Fig. S6 (top) Temperature dependence of the ac susceptibility at different applied dc fields for **1**. (Bottom) Argand plot at various temperatures for **1**. The data shown in black were collected without an applied dc field, while the data shown in red were collected at 2 K with an applied field of 1200 Oe.

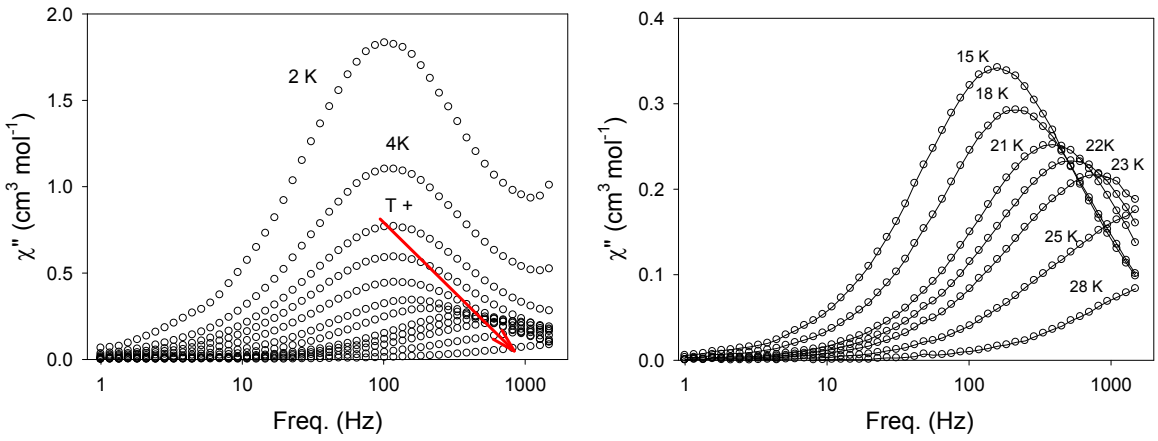

Fig. S7 Out-of-phase susceptibility for **1** as a function of frequency at different temperatures (2-28 K).

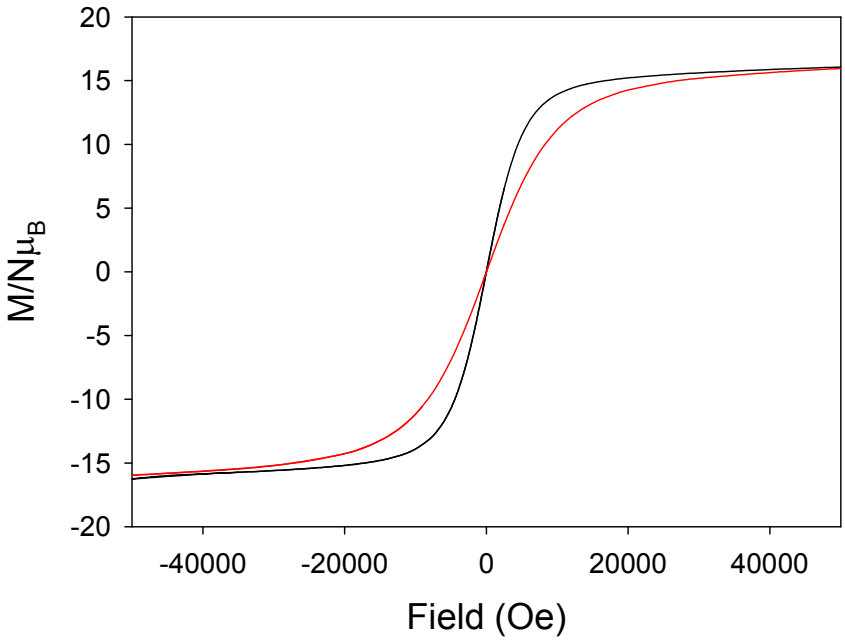

Fig. S8 Magnetization vs. field plot for **1** at 2 K (black) and 4 K (red).